

PAPER • OPEN ACCESS

The preparation of NASICON-type solid electrolyte lithium-ion $\text{Li}_{1+x}\text{Al}_x\text{Ge}_{0.2}\text{Ti}_{1.8-x}(\text{PO}_4)_3$ by conventional solid-state method

To cite this article: X F Shang *et al* 2019 *IOP Conf. Ser.: Mater. Sci. Eng.* **504** 012045

View the [article online](#) for updates and enhancements.

The preparation of NASICON-type solid electrolyte lithium-ion $\text{Li}_{1+x}\text{Al}_x\text{Ge}_{0.2}\text{Ti}_{1.8-x}(\text{PO}_4)_3$ by conventional solid-state method

X F Shang, J H Zhang, S Cheng and Y W Wang

Department of Physics, Faculty of Science, Jiangsu University, Zhenjiang, Jiangsu, 212013, China

Corresponding email: X F Shang, shangxuefu@yeah.net

Abstract. NASICON-type lithium-ion conducting solid electrolyte for $\text{Li}_{1+x}\text{Al}_x\text{Ge}_{0.2}\text{Ti}_{1.8-x}(\text{PO}_4)_3$ were prepared with solid-state method at 900 °C for 7 h. In this paper, we have studied the property of $\text{Li}_{1+x}\text{Al}_x\text{Ge}_{0.2}\text{Ti}_{1.8-x}(\text{PO}_4)_3$ solid electrolyte systems with various numbers of Al replaced Ti. The highest total electrical conductivity of the sintered pellets for $\text{Li}_{1.45}\text{Al}_{0.45}\text{Ge}_{0.2}\text{Ti}_{1.35}(\text{PO}_4)_3$ at 25 °C was 1.0×10^{-3} S/cm, which has NASICON-type crystalline structure without impurity phase. And the sintered pellet as $x=0.45$ in $\text{Li}_{1+x}\text{Al}_x\text{Ge}_{0.2}\text{Ti}_{1.8-x}(\text{PO}_4)_3$ systems also has highest relative density of 95.6% and highest three-point strength of 90 N mm^{-2} , respectively.

1. Introduction

Rechargeable lithium-air battery is a promising power for electric vehicles, because its theoretical energy density is much higher than that of traditional batteries and the cost of materials is lower [1, 2]. Up to now, the two types of lithium-air batteries widely studied and reported by researcher are non-aqueous lithium-air battery and aqueous lithium-air battery respectively. Although the energy density of the lithium-air battery in the aqueous system is lower than that of the non-aqueous battery, it can overcome the defects of the non-aqueous lithium-air battery, such as the corrosion of Li metal by the water and carbon dioxide in the open air environment, the precipitate of the reaction products with high resistance in the discharge process and the high polarization of the Li_2O_2 . In the lithium-air battery of aqueous system, due to the violent reflection of the lithium metal in the water solution, a solid electrolyte of lithium ion conductor is needed as the protective layer to isolate the lithium electrode from the aqueous electrolyte and the external environment [3, 4].

At present, the electrolytes widely studied by researcher mainly have polysulfide, perovskite-type ($\text{Li}_{3x}\text{La}_{2/3-x}\text{B}_{1/3-2x}\text{TiO}_3$), garnet-type ($\text{Li}_7\text{La}_2\text{Zr}_2\text{O}_{12}$), LISICON, NASICON, wherein, NASICON-type solid electrolyte not just have high lithium-ion conductivity but also exhibit water-stable and lowest activation energy for lithium-ion migration [5, 6]. In 1976, Goodenough designed a three-dimensional network structure possessed suitable channels for sodium-ion migration and called this system fast Na-ion conductor [7]. The structure of NASICON-type electrolyte is formed of PO_4 tetrahedron and MO_6 octahedron linked by their corners. The Li ions occupy two positions in conduction channels, one M_1 sites are full occupied by Li ion, but M_2 sites are holes and when Ti ion by substitution of trivalent ion the M_2 sites start to be filled Li ion [8, 9]. The migration path of Li ion in skeleton structure of



NASICON-type electrolyte is speculated along M_1 - M_2 - M_1 sites. The conductivity of NASICON-type electrolyte maybe is related to ionic concentration and migration rate, M_2 sites filled with Li ion by the way of the trivalent ion replaced Ti site can open the bottleneck width [10].

In 1990, Aono reported tetravalence Ti^{4+} in $LiTi_2(PO_4)_3$ system partially was replaced by the trivalent ion such as Al^{3+} , Cr^{3+} , Ga^{3+} , Fe^{3+} , Sc^{3+} , In^{3+} , Lu^{3+} , Y^{3+} , and La^{3+} and found that the conductivity of $Li_{1+x}M_xTi_{2-x}(PO_4)_3$ system can be enhanced and the highest conductivity of 7×10^{-4} S/cm was observed in room temperature when $x=0.3$ and M is Al or Sc. The result of enhanced conductivity was mainly attributed to the grain boundary rather than bulk boundary [11, 12]. All the time, researchers have been trying to improve the grain boundary conductivity of NASICON solid electrolytes by replacing the sites of crystal structure in the $LiTi_2(PO_4)_3$ system by the alternative valence ions. The NASICON type NASICON electrolyte $Li_{1.3}Al_{0.3}Ti_{1.7}(PO_4)_3$ (LATP) [13] and $Li_{1.5}Al_{0.5}Ge_{1.5}(PO_4)_3$ (LAGP) [14] ceramics obtained by the substitution of Al^{3+} and Ge^{3+} for Ti^{4+} have the higher conductivity of 10^{-4} S/cm, which greatly reduces the grain boundary impedance of the electrolyte. Especially for $Li_{1.5}Al_{0.5}Ge_{1.5}(PO_4)_3$ solid electrolyte, the conductivity of the sample reached 4.62×10^{-4} S/cm [14], but the preparation of LAGP was complex, the mechanical strength of the samples was low and the germanium salt was expensive. Maddonado-Manso et al. reported that the solid electrolyte $Li_{1+x}Al_xGe_yTi_{2-x-y}(PO_4)_3$ (LAGTP) samples were obtained by Al^{3+} partial substitution of Ti^{4+} in the LAGP system. The substitution of Al^{3+} made the mechanical strength and electrical conductivity of the sample increased [15]. Zhang et al. reported the precursor of $Li_{1.4}Al_{0.4}Ge_xTi_{1.6-x}(PO_4)_3$ synthesized by sol-gel method, the pellets were sintered at $900^\circ C$ for 11 h and the maximal total conductivity of sintered pellet for $Li_{1.4}Al_{0.4}Ge_xTi_{1.6-x}(PO_4)_3$ was 1.3×10^{-3} S/cm at $25^\circ C$ when $x=0.2$ [16]. Additionally, The LAGTP composite film modified with epoxy resin as the protective film of lithium metal electrode in the aqueous lithium-air battery not only avoid water penetration completely, but also show good chemical stability in the saturated solution of LiCl and LiOH, and have a high conductivity of 5.26×10^{-4} S/cm at room temperature [17]. Xu also have studied the $Li_{1.4}Al_{0.4}Ge_xTi_{1.6-x}(PO_4)_3$ glass ceramics prepared by solid-state method and obtained highest conductivity of 6.12×10^{-4} S/cm at room temperature [18]. In this paper, we prepared the $Li_{1+x}Al_xGe_{0.2}Ti_{1.8-x}(PO_4)_3$ solid electrolyte by the solid-state method and studied their physical and electro-chemical characteristics.

2. Experimental

The precursor of $Li_{1+x}Al_xGe_{0.2}Ti_{1.8-x}(PO_4)_3$ was prepared with conventional solid-state method. Stoichiometric amounts of Li_2CO_3 , TiO_2 , GeO_2 , Al_2O_3 , and $NH_4H_2PO_4$ were ball-milled with Zirconia balls in a zirconia vessel for 2 h at 400 rpm by high-energy mechanical milling (HEMM) with a planetary micro mill after adding alcohol. The obtained mixed powders were pressed into pellets at 150MPa and calcined at $600^\circ C$ for 4 h, then the obtained products were added alcohol for ball milling by HEMM for 4 h after the pellets were reground and press into pellets at 150MPa. The obtained pellets were sintered at $900^\circ C$ for 4 h. After that, the pellets were finely powdered in an agate mortar and the powder was added alcohol for ball milling for 12 h. Finally, the powder was made tablets and sintered at $900^\circ C$ for 7 h.

The phases analysis was operated by a Rigaku Rint 2500 diffractometer with Cu $K\alpha$ radiation in the 2θ range from 10° to 90° at a scanning step rate of $0.02^\circ/s$ as X-ray diffraction (XRD) analysis. The relative densities of $Li_{1+x}Al_xGe_{0.2}Ti_{1.8-x}(PO_4)_3$ pellets were measured by calculating the the ratio of theoretical densities and actual measurement densities. The samples both side were sputtered a thin gold layer as electrodes, then the electrical conductivity of pellets with sputtered gold electrodes were measured by an impedance phase analyzer in the frequency range of 0.1 Hz-1 MHz with the bias voltage at 10mV. The bulk and grain boundray conductivity of samples were calculated from complex plots by Zview 2. Three-point bending strength of LATP samples was measured at room temperature by a materials tester (Shimadzu EX-SX 500 N). The obtained dates for different x were compared and discussed.

3. Results and discussion

Figure 1 shows the XRD patterns of the $\text{Li}_{1+x}\text{Al}_x\text{Ge}_{0.2}\text{Ti}_{1.8-x}(\text{PO}_4)_3$ ($x=0.4, 0.45, 0.5$ and 0.55) pellets sintered at $900\text{ }^\circ\text{C}$ for 7 h. In the condition $x=0.55$, the many impurity phases such as AlPO_4 , LiGe_2O_7 , $\text{LiGe}_2(\text{PO}_4)_3$ and GeP_2O_7 were observed and $x=0.5$, just the impurity phases of Li_3PO_4 were observed, however the samples are pure for lattice structure when $x=0.4$ and 0.45 . All diffraction lines of the samples sintered at $900\text{ }^\circ\text{C}$ for 7 h were accordance with the NASICON-type structure. In previous study, Xu reported $\text{LiGe}_2(\text{PO}_4)_3$ and $\text{LiTi}_2(\text{PO}_4)_3$ phases were observed in $\text{LiGe}_{1-x}\text{Ti}_x(\text{PO}_4)_3$ specimens and no new peak appear, but when $x \geq 0.5$ AlPO_4 impurity phase began to appear [18].

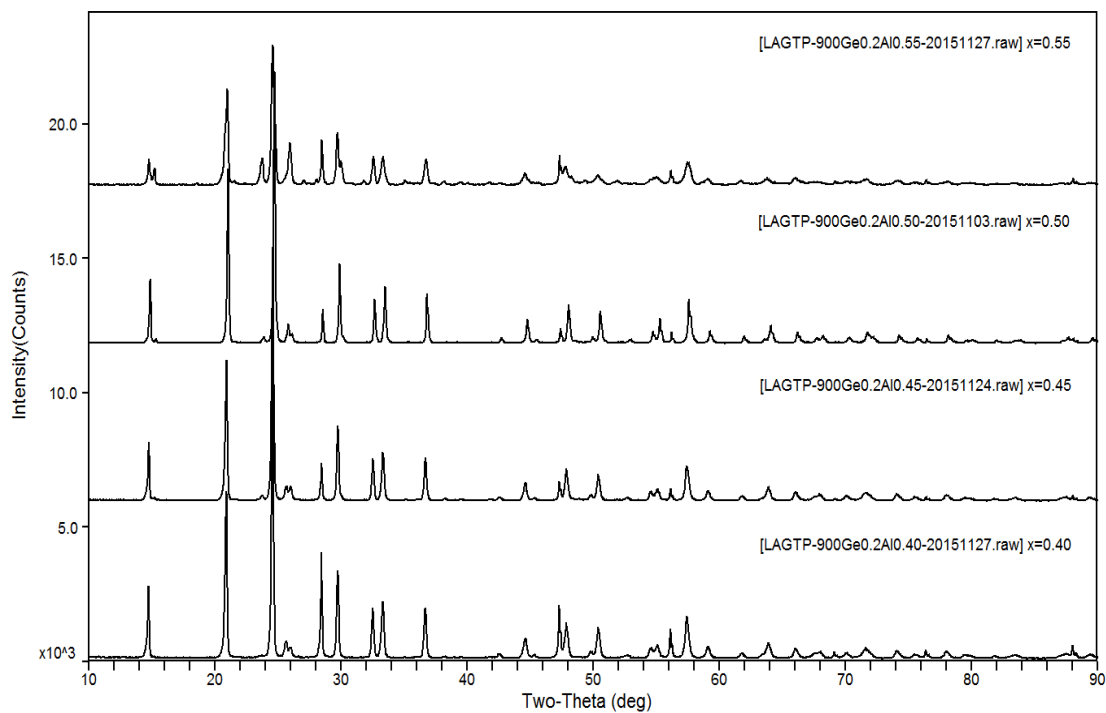


Figure 1. XRD patterns of $\text{Li}_{1+x}\text{Al}_x\text{Ge}_{0.2}\text{Ti}_{1.8-x}(\text{PO}_4)_3$ as the function of x ($x=0.4, 0.45, 0.5$ and 0.55).

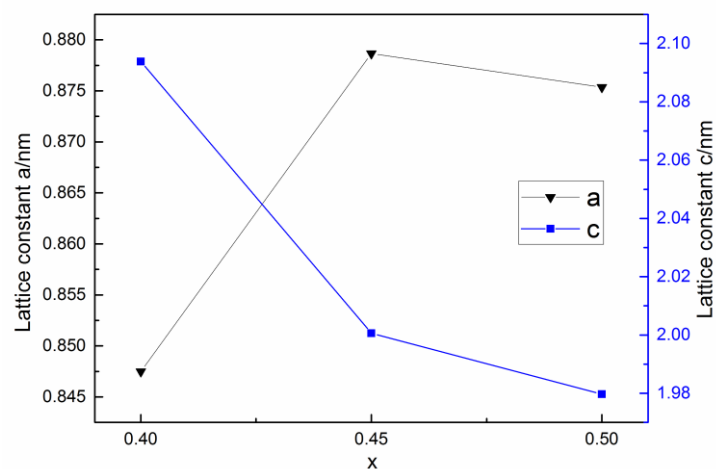


Figure 2. The curves of the lattice parameter with x for $\text{Li}_{1+x}\text{Al}_x\text{Ge}_{0.2}\text{Ti}_{1.8-x}(\text{PO}_4)_3$ samples at room temperature ($x=0.4, 0.45, 0.5$).

Figure 2 shows the changes of the lattice parameters with x for $\text{Li}_{1+x}\text{Al}_x\text{Ge}_{0.2}\text{Ti}_{1.8-x}(\text{PO}_4)_3$ pellets at room temperature. With x from 0.4 to 0.45, the lattice parameter of a was increased from 0.848 Å to 0.877 Å but the lattice parameter of c was decreased from 2.09 Å to 1.99 Å. However, when $x > 0.45$ the lattice parameters of a and c were all decreased. Aono found the lattice parameters were decreased with increasing x in $\text{Li}_{1+x}\text{Al}_x\text{Ti}_{2-x}(\text{PO}_4)_3$ systems, this result is attributed to the substitution of Al^{3+} with smaller ionic radius (0.53nm) for Ti^{4+} with larger ionic radius (0.605nm) [11]. However, the changes of the lattice parameters for $\text{Li}_{1+x}\text{Al}_x\text{Ge}_{0.2}\text{Ti}_{1.8-x}(\text{PO}_4)_3$ systems are not fit with this description of preceding part, it is inferred that the exist of two phases in $\text{Li}_{1+x}\text{Al}_x\text{Ge}_{0.2}\text{Ti}_{1.8-x}(\text{PO}_4)_3$ [16, 18].

Figure 3 shows the relative densities of $\text{Li}_{1+x}\text{Al}_x\text{Ge}_{0.2}\text{Ti}_{1.8-x}(\text{PO}_4)_3$ series pellets sintered at 900 °C for 7 h with different x . The relative densities of sintered pellets were increased with x until $x=0.45$ and start to decline. The highest relative density of sintered pellet is 95.6% when $x=0.45$, which is higher the relative density of 94.4% for LAGTP pellets synthesized by sol-gel method and Shang also reported the highest relative density of 95.5% for LAGTP pellets by solid-state method [16, 19].

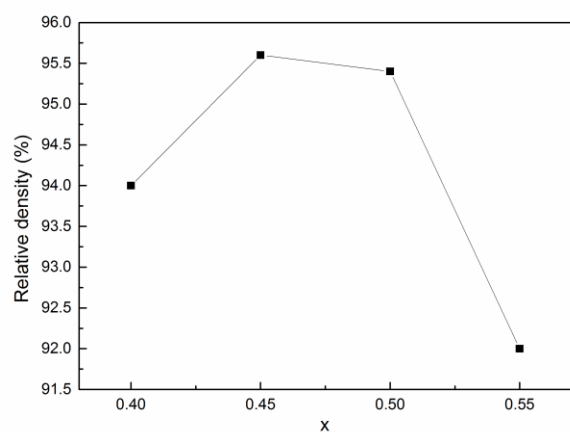


Figure 3. The curves of the relative density for $\text{Li}_{1+x}\text{Al}_x\text{Ge}_{0.2}\text{Ti}_{1.8-x}(\text{PO}_4)_3$ with x ($x=0.4, 0.45, 0.5$ and 0.55).

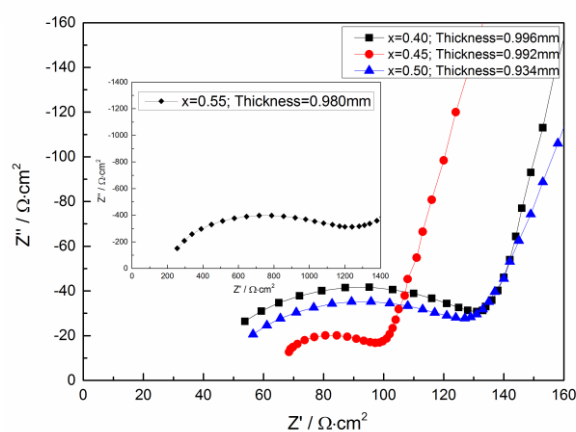


Figure 4. The curves of the impedance patterns for $\text{Li}_{1+x}\text{Al}_x\text{Ge}_{0.2}\text{Ti}_{1.8-x}(\text{PO}_4)_3$ with x ($x=0.4, 0.45, 0.5$ and 0.55).

J. Fu synthesized $\text{Li}_{1+x}\text{Al}_x\text{Ti}_{2-x}(\text{PO}_4)_3$ (LATP) pellets by conventional melt-quenching method, and deeply studied the ionic conductivity of LATP pellets. The bulk resistance and grain boundary resistance of LATP pellets could be obtained by the analysis of EIS graph, the intercept of the semicircle on the real axis at high frequency represents the bulk resistance, the diameter of the semicircle indicates the grain boundary resistance [20]. Figure 4 shows the complex impedance profiles of samples for $\text{Li}_{1+x}\text{Al}_x\text{Ge}_{0.2}\text{Ti}_{1.8-x}(\text{PO}_4)_3$ synthesized with solid-state method as a function of x at 25°C. Only one large semicircle was observed and a straight line follow it. It's consistent with the research of J. Fu. The exist of semicircle is because of grain boundaries, the impedance plots would be managed a suitable equivalent circuit consist of two parallel combination of resistance, capacitance and constant phase element in series [21]. The impedance of sintered pellets for $\text{Li}_{1+x}\text{Al}_x\text{Ge}_{0.2}\text{Ti}_{1.8-x}(\text{PO}_4)_3$ were increased until $x=0.45$, it is that due to the substitute of Al^{3+} for Ti^{4+} in $\text{Li}_{1+x}\text{Al}_x\text{Ti}_{2-x}(\text{PO}_4)_3$ systems would open the bottleneck width [10]. After $x \geq 0.45$, the increasing grain boundary impedance of sintered pellets maybe contribute to the appearance of impurity phase from the inference of XRD patterns.

Aono et al referred that one of important effect for conductivity of $\text{Li}_{1+x}\text{M}_x\text{Ti}_{2-x}(\text{PO}_3)_4$ system is attribution to the relative density [22,23]. Figure 5 shows the total conductivities of $\text{Li}_{1+x}\text{Al}_x\text{Ge}_{0.2}\text{Ti}_{1.8-x}(\text{PO}_4)_3$ as a function of the substitute content of Al^{3+} for Ti^{4+} , the variation trend is same with Figure 3, our experimental data fit with the the consequence of Aono [15]. The highest total

conductivity of 1.0×10^{-3} S/cm were observed for $\text{Li}_{1.45}\text{Al}_{0.45}\text{Ge}_{0.2}\text{Ti}_{1.35}(\text{PO}_4)_3$ at $x=0.45$. Previously, Maddonado-Manso reported the highest total conductivity reached 7×10^{-4} S/cm for $\text{Li}_{1+x}\text{Al}_x\text{Ge}_y\text{Ti}_{2-x-y}(\text{PO}_4)_3$ series. The highest conductivity of 1.3×10^{-3} S/cm was measured at 25°C for $\text{Li}_{1+x}\text{Al}_x\text{Ge}_y\text{Ti}_{2-x-y}(\text{PO}_4)_3$ pellets synthesized by sol-gel method when $x=0.2$ and $y=0.4$ by Zhang [16], which is slightly higher than been this sample prepared by solid-state method.

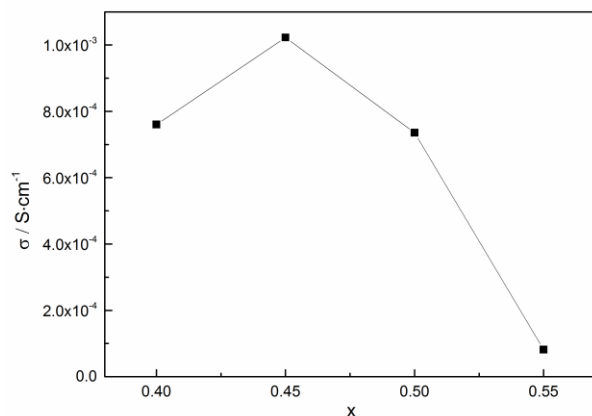


Figure 5. the curve of the total conductivity for $\text{Li}_{1+x}\text{Al}_x\text{Ge}_{0.2}\text{Ti}_{1.8-x}(\text{PO}_4)_3$ with x ($x=0.4, 0.45, 0.5$ and 0.55).

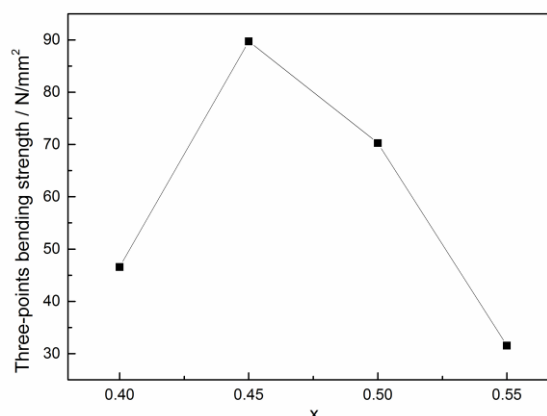


Figure 6. The curve of the three-point bending strength for $\text{Li}_{1+x}\text{Al}_x\text{Ge}_{0.2}\text{Ti}_{1.8-x}(\text{PO}_4)_3$ with x ($x=0.4, 0.45, 0.5$ and 0.55).

Figure 6 shows the three-point bending strength of $\text{Li}_{1+x}\text{Al}_x\text{Ge}_y\text{Ti}_{2-x-y}(\text{PO}_4)_3$ pellets prepared by solid-state method related to x at 25°C [17]. The maximum bending strength of 90 N mm^{-2} was measured for $\text{Li}_{1.45}\text{Al}_{0.45}\text{Ge}_{0.2}\text{Ti}_{1.35}(\text{PO}_4)_3$, which is higher than the maximum bending strength of 65 N mm^{-2} for $\text{Li}_{1.4}\text{Al}_{0.4}\text{Ti}_{1.4}\text{Ge}_{0.2}(\text{PO}_4)_3$ films prepared by sol-gel method by Zhang.

4. Conclusions

The precursor of water-stable lithium-ion conducting solid electrolyte $\text{Li}_{1+x}\text{Al}_x\text{Ge}_y\text{Ti}_{2-x-y}(\text{PO}_4)_3$ series prepared by solid-state method, the pressure forming pellets were sintered at 900°C for 7 h. the highest conductivity of 1.0×10^{-3} S/cm for $\text{Li}_{1.45}\text{Al}_{0.45}\text{Ti}_{1.35}\text{Ge}_{0.2}(\text{PO}_4)_3$ was obtained at 25°C and the sample was the purity phase by XRD pattern analysis as $x=0.45$, the lattice parameters a and c of $\text{Li}_{1.45}\text{Al}_{0.45}\text{Ti}_{1.35}\text{Ge}_{0.2}(\text{PO}_4)_3$ are 0.877 \AA and 1.990 \AA , respectively. A three-point bending strength of 90 N mm^{-2} was measured and the relative density was 95.6% for $\text{Li}_{1.4}\text{Al}_{0.4}\text{Ti}_{1.4}\text{Ge}_{0.2}(\text{PO}_4)_3$ sintered pellet at 25°C . The NASICON-type LAGTP sintered pellets prepared by solid-state method have a approximative lithium-ion conducting property and better mechanical strength contrasted with the NASICON-type LAGTP prepared by sol-gel method and melt-quenching method, but the solid-state method has the advantage of simple preparation process, low cost and easy to mass production for practical application. The LAGTP samples prepared by conventional solid-state method have highlight performance for promising candidate of solid electrolyte in the Li-S battery, all-solid-state battery and Li-air battery application.

Acknowledgments

The authors gratefully acknowledge the financial supports from the National Natural Science Foundation of China (11304125) and the Research Foundation for Advanced Talents, Jiangsu University (10JDG077).

References

- [1] Armand M and Tarascon J M 2008 Building better batteries *Nature* Vol 451 No 7 pp 652-657
- [2] Tarascon J M and Armand M 2001 Issues and challenges facing rechargeable lithium batteries

- Nature* Vol 414 No 15 pp 359-367
- [3] Visco S J, Nimon E, Katz B, Jonghe L D and Chu M Y 2006 The Development of High Energy Density Lithium/Air and Lithium/Water Batteries with No Self-Discharge *Electrochemical Society*
- [4] Zhang T, Imanishi N, Shimonishi Y, Hirano A and Takeda Y 2010 A novel high energy density rechargeable lithium/air battery *Chem. Commun.* Vol 46 pp 1661-1663
- [5] Asachi G, Imanaka N and Aono H 1996 Fast Li⁺ conducting ceramic electrolytes *Adv. Mater.* Vol 8 No 2 pp 127-135
- [6] Knauth P 2009 Inorganic solid Li ion conductors: An overview *Solid State Ionics* Vol 180 No 14 pp 911-916
- [7] Goodenough J B, Hong H Y-P and Kafalas J A 1976 Fast Na⁺-ion transport in skeleton structures *Mat. Res. Bull* Vol 11 pp 203-220
- [8] Losilla E R, Aranda M A G, Bruque S, Paris M A, Sanz J and West A R 1998 Understanding Na mobility in NASICON materials: a rietveld ²³Na and ³¹P MAS NMR and impedance study *Chem. Mater.* Vol 10 pp 665-672
- [9] Martinez-Juarez A, Pecharroman C, Iglesias J E and Rojo J M 1998 Relationship between activation energy and bottleneck size for Li⁺ ion conduction in NASICON materials of composition LiMM'(PO₄)₃; M, M'=Ge, Ti, Sn, Hf *J. Phys. Chem. B.* Vol 102 pp 372-375
- [10] Nuspi G, Takeuchi T, Weiß A, Kageyama H, Yoshizawa K and Yamabe T 1999 Lithium ion migration pathway in LiTi₂(PO₄)₃ and related materials *J. Appl. Phys.* Vol 86 No 10 pp 5484-5491
- [11] Aono H, Sugimoto E, Sadaoka Y, Imanaka N and Adachi G 1990 Electrical properties of sintered lithium titanium phosphate ceramics (Li_{1+x}M_xTi_{2-x}(PO₄)₃, M³⁺=Al³⁺, Sc³⁺, or Y³⁺) *Chem. Lett.* pp 1825-1828
- [12] Aono H, Sugimoto E, Sadaoka Y, Imanaka N and Adachi G 1990 Ionic conductivity of solid electrolytes based on lithium titanium phosphate *J. Electrochem. Soc* Vol 137 No 4 pp 1023-1027
- [13] Ma F, Zhao E, Zhu S, Yan W, Sun D, Jin Y and Nan C 2016 Preparation and evaluation of high lithium ion conductivity Li_{1.3}Al_{0.3}Ti_{1.7}(PO₄)₃ solid electrolyte obtained using a new solution method *Solid State Ionics* Vol 295 pp 7-12
- [14] Thokchom J S, and Kumar B 2008 Composite effect in superionically conducting lithium aluminium germanium phosphate based glass-ceramic *Journal of Power Sources* Vol 185 No 1 pp 480-485
- [15] Maldonado-Manso P, Losilla E R, Martinez-Lara M, Aranda M A G, Bruque S, Mouahid F E and Zahir M 2003 High lithium ionic conductivity in the Li_{1+x}Al_xGe_yTi_{2-x-y}(PO₄)₃ NASICON series *Chem. Mater.* Vol 15 pp 1879-1885
- [16] Zhang P, Matsui M, Hirano A, Takeda Y, Yamamoto O and Imanishi N 2013 Water-stable lithium ion conducting solid electrolyte of the Li_{1.4}Al_{0.4}Ti_{1.6-x}Ge_x(PO₄)₃ system (x=0-1.0) with NASICON-type structure *Solid State Ionics* Vol 253 pp 175-180
- [17] Zhang P, Wang H, Lee Y, Matsui M, Takeda Y, Yamamoto O and Imanishi N 2015 Tape-cast water-stable NASICON-type high lithium ion conducting solid electrolyte films for aqueous lithium-air batteries *J. Electrochem. Soc.* Vol 162 No 7 pp A1265-A1271.
- [18] Xu X X, Wen Z Y, Gu Z G, Xu X H and Lin Z X 2004 Lithium ion conductive glass ceramics in the system Li_{1.4}Al_{0.4}(Ge_{1+x}Ti_x)_{1.6}(PO₄)₃ (x=0-1.0) *Solid State Ionics* Vol 171 pp 207-213.
- [19] Shang X F, Nemori H, Mitsuoka S, Xu P, Matsui M, Takeda Y, Yamamoto O and Imanishi N 2016 High lithium-ion conducting NASICON-type Li_{1+x}Al_xGe_yTi_{2-x-y}(PO₄)₃ solid electrolyte *Frontiers in Energy Research* Vol 4 Article 12
- [20] Fu J 1997 Superionic conductivity of glass-ceramics in the system Li₂O-Al₂O₃-TiO₂-P₂O₅ *Solid State Ionics* Vol 96 pp 195-200
- [21] Kazakevicius E, Urcinskas A, Keziionis A, Dindune A, Kanepe Z and Ronis J 2006 Electrical properties of Li_{1.3}Ge_{1.4}Ti_{0.3}Al_{0.3}(PO₄)₃ superionic ceramics *Electrochimica. Acta.* Vol 51 pp

6199-6202

- [22] Aono H, Sugimoto E, Sadaoka Y, Imanaka N and Adachi G 1989 Ionic conductivity of the lithium titanium phosphate ($\text{Li}_{1+x}\text{M}_x\text{Ti}_{2-x}(\text{PO}_4)_3$, M=Al, Sc, Y, and La) systems *J. Electrochem. Soc.* Vol 136 No 2 pp 590-591
- [23] Aono H, Sugimoto E, Sadaoka Y, Imanaka N and Adachi G 1993 The electrical properties of ceramic electrolytes for $\text{LiM}_x\text{Ti}_{2-x}(\text{PO}_4)_3+y\text{Li}_2\text{O}$, M=Ge, Sn, and Zr systems. *Journal of the Electrochemical Society* Vol 140 No 7 pp 1827-1833